

# INFLUENCE OF INJECTION MOLDING PARAMETERS ON THE SURFACE STRUCTURE OF POLYAMIDE PARTS

*Marius Janßen, Mirco Janßen, Reinhard Schiffers and Robin Blankenagel,  
University of Duisburg-Essen, Institute of Product Engineering (ipe), Duisburg, Germany  
Felix Heinzler and Marvin Wagner,  
BIA Kunststoff- und Galvanotechnik GmbH & Co. KG, Solingen, Germany*

## Abstract

Injection molded and then electroplated plastic parts are mainly made of acrylonitrile butadiene styrene (ABS) or polycarbonate/acrylonitrile butadiene styrene (PC/ABS) blends. Nevertheless, compared to these materials, polyamide (PA) has superior physical properties. However, the coating quality is inferior to that of conventional polymers and the scrap rates of 25% to 30% are higher. The coating quality depends not only on the electroplating parameters but also on the surface of the injection molded part.

The aim of this paper is to determine the influence of injection molding parameters on the surface structure of injection molded, mineral-filled polyamide parts. Therefore, mineral-filled polyamide parts are produced in a full-factorial design of experiments (DoE) and electroplated subsequently. Afterwards, surface parameters from DIN EN ISO25178 are determined by confocal microscopy for different pre-treatments of the electroplating process chain and at different positions.

## Introduction

Injection molded and subsequently electroplated plastic parts are highly relevant for the automotive industry in interior and exterior applications [1]. These hybrid material composites enhance the visual and haptic appearance and replace common metal parts.

Besides conventional electroplated materials like ABS or PC/ABS blends, mineral-filled PA is used, because of superior physical properties. For instance, PA has a higher stiffness, hardness and heat distortion temperature [2]. Unfortunately, the scrap rate for PA is very high at up to 30% - three times higher than for ABS [3]. The defects, such as uneven gloss or insufficient adhesion between the plastic part and the metal layer, are usually only apparent in the final product [3]. The injection molding process has a major influence on the surface and subsurface of the part and thus on the adhesion strength and the appearance [4]. The part geometry, material properties and injection molding parameters, such as injection speed, are particularly important factors for ABS [2, 4, 6, 7]. The main cause of the optical defects is the high mineral content and the reaction of the material to the processing conditions. In

this article a systematic investigation of the influence of the injection molding process on the surface of the polyamide part is presented to evaluate which factors have an influence on mineral-filled PA.

## Electroplating of Polyamides

In principle, the electroplating of polymers (here polyamide) is comparable to that of metals. The difference is that polymers require a special electroless pretreatment because of their non-conductive properties [2]. The procedure for electroplating mineral-filled PA 6 is described below, whereby only those steps are described that are necessary prior to the classical electroplating of metals. After injection molding, the part is immersed in an etch containing chromosulfuric acid in a first step. During this process step, PA close to the surface is oxidized and dissolved. Thus, mineral particles are exposed. In a second step, the so-called neutralizer, ultrasound is applied to wash out the etching residues especially the chromosulfuric acid. In a third process step, the so-called conditioner, the exposed mineral particles are attacked or dissolved out in a fluorine-containing immersion bath. A cavernlike surface structure is received. In a fourth step, the structured surface is then covered with palladium in an activator bath. In the following fifth step, catalytic palladium nuclei are generated in an acceleration bath. In the last step, a chemical metal deposition can be carried out, resulting in a thin and electrically conductive nickel layer. A standard electroplating process can then follow, and the component can be coated with further metal layers (e.g. Watts nickel, copper, bright nickel, chrome).

## Surface Parameters

DIN EN ISO 25178-2 contains multiple parameters to characterize 3D-topographies [5]. They can be divided into height, spatial, structure-based, hybrid and functional parameters. This paper focuses on the height and functional parameters. From the group of height parameters,  $S_q$  and  $S_a$  are presented below:

$$S_q = \sqrt{\frac{1}{A} \iint_A z^2(x, y) dx dy} \quad (1)$$

$$S_a = \frac{1}{A} \iint_A |z(x, y)| dx dy \quad (2)$$

where  $A$  is the measured area and  $z(x, y)$  is the height at position  $(x, y)$ .  $S_q$  describes the mean square height in the definition area; whereas,  $S_a$  is the arithmetic mean of the absolute heights in the measured area. The functional volume parameters are based on the areal-material ratio curve (also called Abbot-Firestone curve) [5].  $V_{mc}$  describes the core material volume by the difference between the area-related material volumes of 10% and 80%. Analogously,  $V_{vc}$  describes the core void volume. For a detailed calculation see [5]. The number of motifs, in this case the number of valleys, is to be used as a further key figure. Using segmentation by applying the watershed algorithm, certain motifs such as valleys and hills can be found [5].

## Experimental Setup

Figure 1 shows the symmetrical plate specimen, which is used to carry out the experimental studies. Furthermore, the positions (PO) at which the surface characteristics will be measured are shown. The experiments are carried out on a KraussMaffei 120-380 PX injection molding machine with a 40 mm diameter three-zone screw. The mold made by Axxicon Moulds Eindhoven B.V. has a mirror polished surface. The material used is a 40% mineral-filled PA 6 (Minlon 73M40 NC010, DuPont de Nemours, Inc., Wilmington, DE, USA). In order to achieve the prescribed residual moisture of  $< 0.2\%$ , the material was dried with a dry air oven at  $80^\circ\text{C}$  for 2.75 hours. The moisture content in the experiment was  $0.03\%$ .

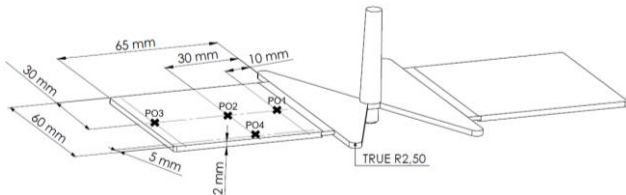


Figure 1. Symmetrical plate shaped specimen with measurement positions (PO).

To investigate the influence of process parameters on the surface, three essential process parameters are systematically varied in a design of experiments (DoE). The barrel temperature, the cooling temperature and the screw advance speed are varied around a center point (0) at two levels (+/-) (Table 1) in a  $2^{3+1}$  experimental design (Table 2). The selection of the parameters is based on an extensive literature research [2, 4, 6, 7].

Table 1. Factor levels of the  $2^{3+1}$  design of experiments.

Factors		Factor levels		
ID	Setting value	(-)	(0)	(+)
A	barrel temp. [ $^\circ\text{C}$ ]	280	290	300
B	cooling fluid temp. [ $^\circ\text{C}$ ]	70	80	90
C	Screw advance speed [mm/s]	10	20	30

Table 2. Structure of the  $2^{3+1}$  DoE.

Series	Factors or Factor levels		
	A	B	C
S1	-	-	-
S2	-	-	+
S3	-	+	-
S4	-	+	+
S5	+	-	-
S6	+	-	+
S7	+	+	-
S8	+	+	+
S9	0	0	0

The screw advance speed is not constant but varies with the screw position. The injection profile is presented in Figure 2.

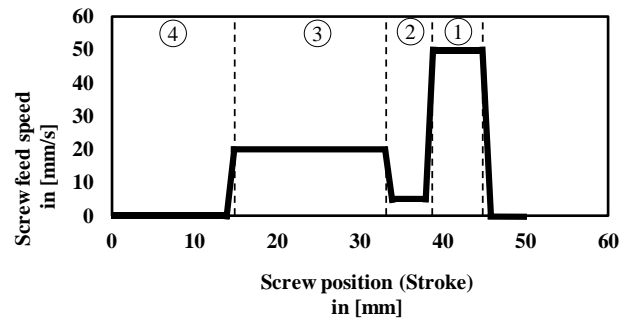


Figure 2. Injection profile for the experiments (right to left).

The aim is a steady flow front velocity in order to obtain a high surface quality. With a screw advance speed of 50 mm/s in stage 1 a complete closing of the non-return valve shall be ensured. The screw is then moved in stage 2 at a lower speed of 5 mm/s to reduce surface defects and orientation in the gate. After the gates are filled, in stage 3 the screw advance speed is increased to the velocity C. The screw advance speed remains constant until the cavity is filled and the holding pressure phase follows. Consequently, the screw advance speed is only varied in stage 3. All other machine parameters have been kept constant during production, so that only factors A, B and C can influence part quality. During the experiment, it was ensured that the process has stabilized after changing the experimental series. After achieving the stationary state, ten parts were produced for each series. Four parts remained untreated. The other six were fed into the electroplating process chain, with two parts each being removed after the neutralizer and conditioner steps. The remaining two parts were coated with a glossy chrome layer. Consequently, there is no influence of the electroplating parameters but only of the injection molding process.

## Confocal Microscopy

Using confocal measurement technology, high resolution, three-dimensional surface measurements can be carried out and evaluated by the key figures of DIN EN ISO 25175-6 [5]. The system used is a confocal microscope from NanoFocus AG of the  $\mu$ Surf type in combination with a 320S lens, which achieves a magnification of 50x with an area measuring range of  $320 \mu\text{m} \times 320 \mu\text{m}$  and a signal processing of  $512 \times 512$  pixels. Accordingly, a measuring point is recorded every  $0.63 \mu\text{m}$ . To display structures, at least three measuring points are required, so that surface structures with an area of approx.  $3.6 \mu\text{m}^2$  can be recorded. The vertical resolution (also depth resolution), can be as low as 4 nm and is therefore sufficient to characterize the depth structures of the test specimens.

## Results

Subsequently, the influence of the injection molding parameters on the surface parameters is presented. First, it is shown how the pre-treatment steps (neutralizer & conditioner) change the surface characteristics. Then the influence of the injection molding process on the key figures is discussed based on PO 2. Finally, deviating results of other PO will be presented.

### Electroplating pre-treatment

In the following, the influence of the pre-treatment (neutralizer and conditioner) on selected surface parameters will be analyzed. Thus, Figure 3 and 4 show  $S_q$  and  $S_a$  for the different process steps, experimental series and positions.

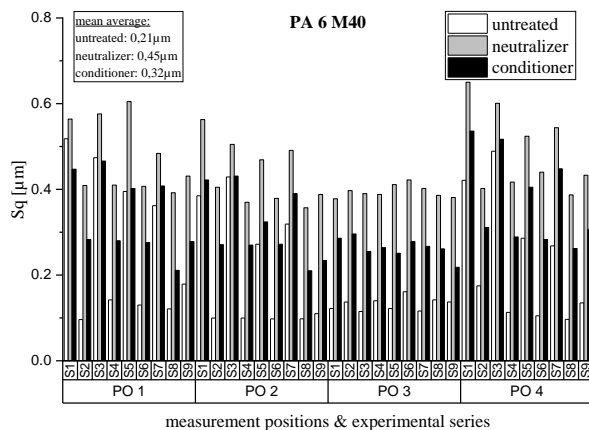


Figure 3.  $S_q$  for different process steps, experimental series and PO.

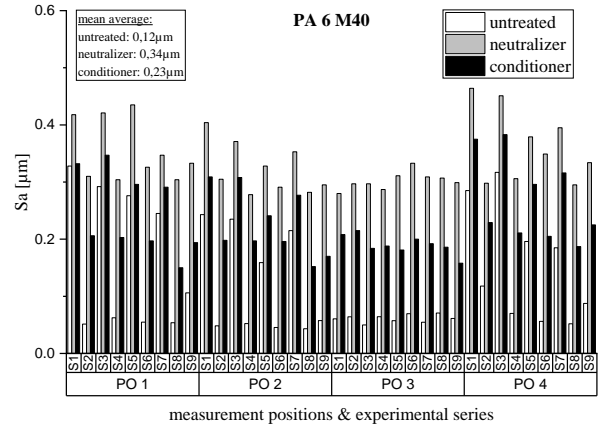


Figure 4.  $S_a$  for different process steps, experimental series and PO.

For  $S_q$ , the mean value across all experimental series and PO of both neutralizer with  $0.45 \mu\text{m}$  and conditioner with  $0.32 \mu\text{m}$  are above the mean value of the untreated surface with  $0.21 \mu\text{m}$ . The same can be found with  $S_a$ . Here, the mean values for untreated are  $0.12 \mu\text{m}$ , neutralizer  $0.34 \mu\text{m}$  and conditioner  $0.23 \mu\text{m}$ . It can be concluded that the etching increases the surface roughness. Since the values of the conditioner are lower than those of the neutralizer, it can be assumed that the topography is smoothed by removing material peaks. The indicators could be used in follow-up investigations to establish a correlation with the metallic surface quality.

### Influence of injection molding parameters

Besides the influence of the pre-treatment stages, the influence of the parameters of the injection molding process will be analyzed with focus on PO 2. This position was exemplarily selected because of its central location. Deviant results of other PO are discussed at the end of the article.

For the parameters  $S_q$  (Figure 5) and  $S_a$  (Figure 6), it can be determined in all three process stages that the experimental series S1, S3, S5 and S7 are above S2, S4, S6 and S8. Taking the factors of the DoE into account, a correlation between the screw advance speed and the residual surface roughness can be concluded. The first group of series represents a low level of the factor C, whereas the second group is characterized by a high level of factor C. It can be assumed that an increase of the screw advance speed and thus the injection speed leads to a reduction of  $S_q$  and  $S_a$ . Nevertheless, no linearity can be determined based on the values of the center point (S9). Considering the small database of the center point, the experiments should be extended to be able to conclude about a possible linearity or non-linearity. No significant effects were found for factors A and B and their interactions.

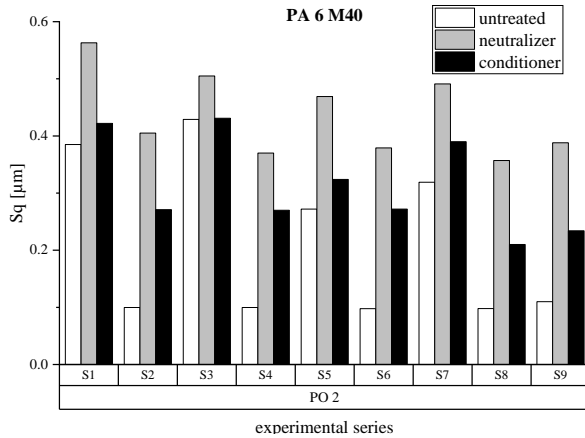


Figure 5.  $S_q$  for different process steps and series at PO 2.

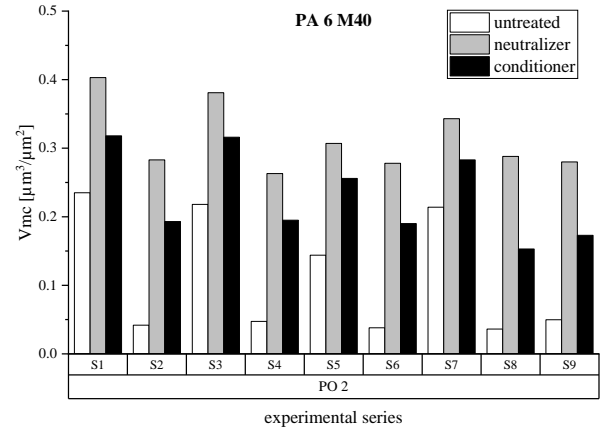


Figure 7.  $V_{mc}$  for different process steps and series at PO 2.

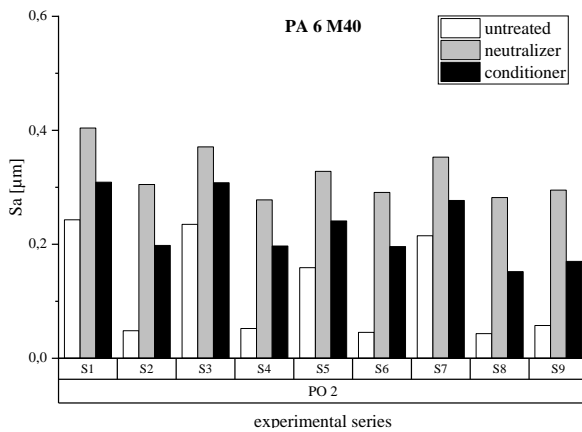


Figure 6.  $S_a$  for different process steps and series at PO 2.

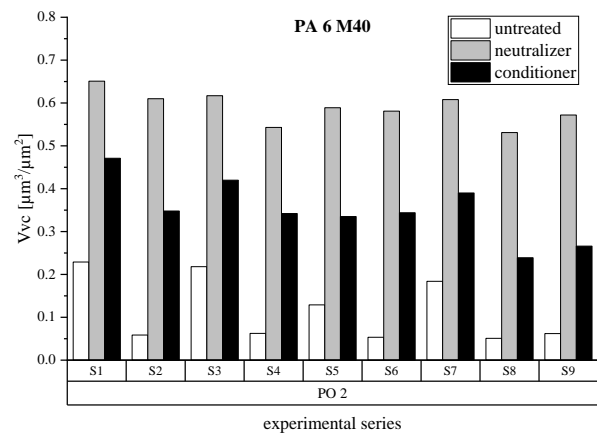


Figure 8.  $V_{vc}$  for different process steps and series at PO 2.

Higher injection speeds result in higher shear loads caused by wall adhesion. Thus, higher orientations of the polymer chains should be obtained [8]. Higher orientations are associated with higher roughness, because the frozen stresses are subject to a stronger etch attack [3]. This would be contrary to the results, but there is also a correlation between the injection speed and the melt temperature. As the injection speed increases, the melt temperature also rises, resulting in slower solidification of the surface layer and a reorientation of the polymer chains [8]. It can be assumed that the effect of reorientation is more significant, and the overall surface roughness is reduced. Furthermore, the higher temperature is associated with the formation of crystalline structures. Since only the amorphous structures are attacked by the etching process [2, 3], a lower surface roughness is achieved.

Figure 7 shows the core material volume for the different process steps at PO2, whereas Figure 8 presents the core void volumes. Similar to  $S_q$  and  $S_a$ , the values of  $V_{mc}$  and  $V_{vc}$  for S1, S3, S5 and S7 are mostly above those of S2, S4, S6, and S8.

It can be derived that the screw advance speed influences the core volume with statistically negative effect direction. Thus, if factor C increases, the core volume decreases and vice versa. As with  $S_q$  and  $S_a$ , there is a superposition of higher shear rates and higher melt temperatures, resulting in slower solidification. Because of the associated reorientation, the surface is smoother, reducing the core material and core void volume caused by fewer tops and valleys. Again, no linearity can be assumed due to the values of S9.

The pre-treatments achieve more core void volumes, which increases the potential for mechanical bonding of the electroless nickel-plated metal layer. However, confocal microscopic results do not allow any conclusions to be drawn about the geometric expansion of e.g. undercuts.

Finally, a result of the motif analysis, namely the number of valleys, is presented in Figure 9. Considering the number of valleys, it can be determined that the experimental series with a high level of factor C produce a larger number of valleys. The results of the motif analysis follow on from this, since it is understandable that finer roughness is also associated with smaller and thus overall,

more motifs. It can be assumed that a higher number of motifs and the associated smaller averaged motif areas lead to a better palladium coating or metallization quality. As with the other key figures, no significant correlation could be found for factors A and B. Moreover, no linearity assumption is possible.

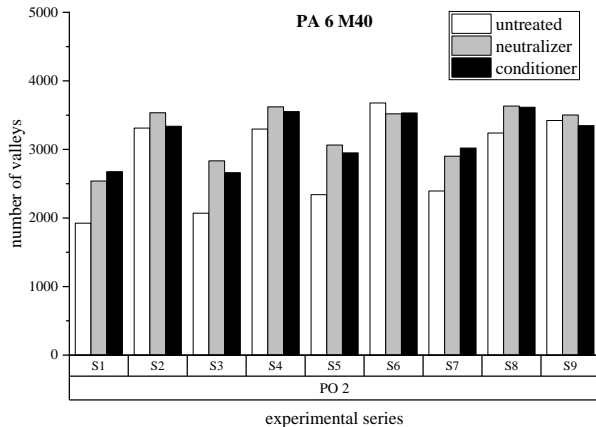


Figure 9. Number of valleys for different process steps and series at PO 2.

## Measurement Positions

Finally, the position on the part and its influence on the surface characteristics will be discussed. Therefore, the similarities and differences between the PO are presented below. For PO1 and PO4 the same relationships can be found as for PO2. With increasing screw advance speed (factor C), the surface roughness as well as the core material and core void volume decreases. Simultaneously, the number of valleys increases.

In contrast, the previous results cannot be confirmed for PO3, resulting in a deviating surface on the PA part. In this case, the factor C has a minor impact on  $S_q$  and  $S_a$  with statistically positive direction. Furthermore, the factor B influences the key figures from the motif analysis. This factor influences the number of valleys with positive and the averaged valley area with negative effect direction. A possible explanation is that the higher mold temperature and the associated slower solidification of the melt results in increased crystallization. However, amorphous structures are required for proper metallization, because crystalline structures cannot be dissolved in the pretreatment [2, 3]. It is possible that the effect of factor B at PO3 only became apparent because there is increased mold contact at this position. This leads to faster cooling, so that an increase in mold temperature has a stronger effect. This would also correspond to the statistically positive direction of factor C. The orientations cannot recede due to the increased wall adhesion, i.e. an increase in the screw advance speed leads to an increase in surface roughness at PO 3.

## Conclusions and Outlook

In order to investigate the influence of the injection molding parameters on the surface of mineral-filled PA, key figures from DIN EN ISO 25178-2 were determined and analyzed using confocal microscopy. The process steps etch and neutralizer significantly increase the surface roughness compared to an untreated part, whereas the conditioner achieves a smoothing effect. The screw advance speed and thus the injection speed were identified as the most decisive factor for the surface structure for all process steps at PO 1, 2 and 4. As the injection speed increases, the surface roughness decreases, which is probably caused by reorientation processes and crystallization. An influence of the mold temperature could also be detected, but only for PO 3.

To validate the results, further measurements could be performed. Conceivable, for instance, would be SEM investigations to generate information about the mineral particles in the surface layer. Of further interest is information about the geometry of the caverns, i.e. about undercuts, which could be achieved by investigations in a sectional plane. The aim of future research is to use multi-phase simulation to identify flow phenomena that influence the formation of the surface layer. Thereby segregations or accumulations of minerals can be identified and correlated with the resulting surface layer.

## Acknowledgements

This research is funded by the Deutsche Forschungsgemeinschaft (DFG, German Research Foundation)– 441824520. This publication was created in the context of this research project.

## References

1. F. Heinzler and P. Weiß, *Kunststoffe*, **08**, 28, (2014).
2. R. Suchentrunk et al., *Kunststoff-Metallisierung*, Leuze Verlag, Bad Saulgau, (2007).
3. M. Lake, *Oberflächentechnik in der Kunststoffverarbeitung: Vorbehandeln, Beschichten, Funktionalisieren und Kennzeichnen von Kunststoffoberflächen*, Carl Hanser Verlag, Munich, (2016).
4. J.P. Siepmann, D. Mazur, J. Wortberg, C. Notthoff and F. Heinzler, *SPE-ANTEC*, Indianapolis, 1096, (2016).
5. DIN EN ISO 25178-2, Geometrical product specifications (GPS) – Surface texture: Areal (ISO 25178-2:2012).
6. J.P. Siepmann, J. Wortberg and F. Heinzler, *SPE-ANTEC*, Anaheim, 1478, (2017).
7. R. Schiffers, J.P. Siepmann, M. Janßen and J. Wortberg, *SPE ANTEC*, Orlando, (2018).
8. F. Johannaber and W. Michaeli, *Handbuch Spritzgießen*, Carl Hanser Verlag, Munich, (2004).

# DuEPublico

Duisburg-Essen Publications online

UNIVERSITÄT  
DUISBURG  
ESSEN

*Offen im Denken*

ub | universitäts  
bibliothek

This text is made available via DuEPublico, the institutional repository of the University of Duisburg-Essen. This version may eventually differ from another version distributed by a commercial publisher.

**DOI:** 10.17185/duepublico/76901

**URN:** urn:nbn:de:hbz:465-20220921-160655-4

This is the **Authors Accepted Manuscript** of an article finally published in: *ANTEC 2021 - Conference Proceedings of the 2021 SPE Annual Technical Conference*. Society of Plastics Engineers, 2021. ISBN 978-1-7138-3075-7, pp. 505-509.

© The authors. All rights reserved.